

# Small-Angle Scattering Analysis of Tetrahedral Particles

## Abstract

An isotropic polydisperse arrangement of homogeneous tetrahedral particles, independently arranged in space and possessing a random edge length  $a$ , has been considered. Models for determining the size distribution density  $f(a)$  (via random intersections of the particles and via their set covariance) have been explained. The starting point is the application of the averaged isotropised set covariance of a single tetrahedron  $C(r)$ . A robust and reliable procedure for handling the resulting equations numerically is presented. As  $C(r)$  is closely connected with the so-called small-angle scattering correlation function  $\gamma(r)$ , the results can also be applied for particle sizing via scattering methods of tetrahedral micro-objects in biology or material science. Indeed, the application of scattering methods does not require image material. However, the particle shape must be known a priori.

**Key words:** stereology, particle size distribution, set covariance, linear intercept measurement, IUR chords, scattering methods, Titchmarsh transformation.

## Introduction

Particle sizing based on the data of measurements of intercept lengths on a random line through many homogeneous particles embedded in a matrix (isotropic two-phase sample) is a basic stereological problem [1]. Important applications of this concept are in material science and biology, beginning at a length scale of several nanometers. The determination of particle size distributions of selected particle shapes from experimental data has already been discussed for a large class of geometric shapes [2,3]. Two basic principles of the measurement exist: on the one hand, particle size distributions of a sequence of well-defined particle shapes can be obtained via pure image analysis [4]. On the other hand, scattering experiments with electromagnetic waves lead to scattering curves, which also include information about the particle sizes [5,6,7].

Basic approaches for a large spectrum of three-dimensional particle shapes (including two-dimensional and one-dimensional limiting cases) are known. Several particle shapes can be handled by use of the so-called Titchmarsh transformation (see [7] and Appendix), which allows the researcher to determine the size distribution density of a characteristic diameter of the particle analytically, if the small-angle scattering intensity of a single prototype of particle is proportional to the square of the Bessel function of the first kind of index  $\nu$ . Unfortunately, analytic solutions based on such special integral transformations are rare and exceptional cases [8]. The tetrahedron case is a very special one, and therefore not included in [8].

This paper considers an isotropic arrangement of tetrahedrons, possessing a random edge length  $a$  (Figure 1). Let the smallest distance between any two tetrahedrons be greater than the longest edge  $a_{\max} = L$  of the greatest tetrahedron. This assumption of a quasi-diluted particle arrangement is useful for the interpretative small-angle scattering (SAS) experiments. Then, the whole scattering intensity is simply the sum of the scattering intensities of all particles. For SAS investigations of samples such as Figure 1, the particle shape must be known. Then, no image material is required to determine the distribution density  $f(a)$ .

After briefly explaining structure functions and theory, the single tetrahedron for a constant edge length  $a$  is the starting point. Then, the averaging procedure is explained for the realistic case of different edge lengths  $a_i$  (Figure 1). Three integral equations result, which connect

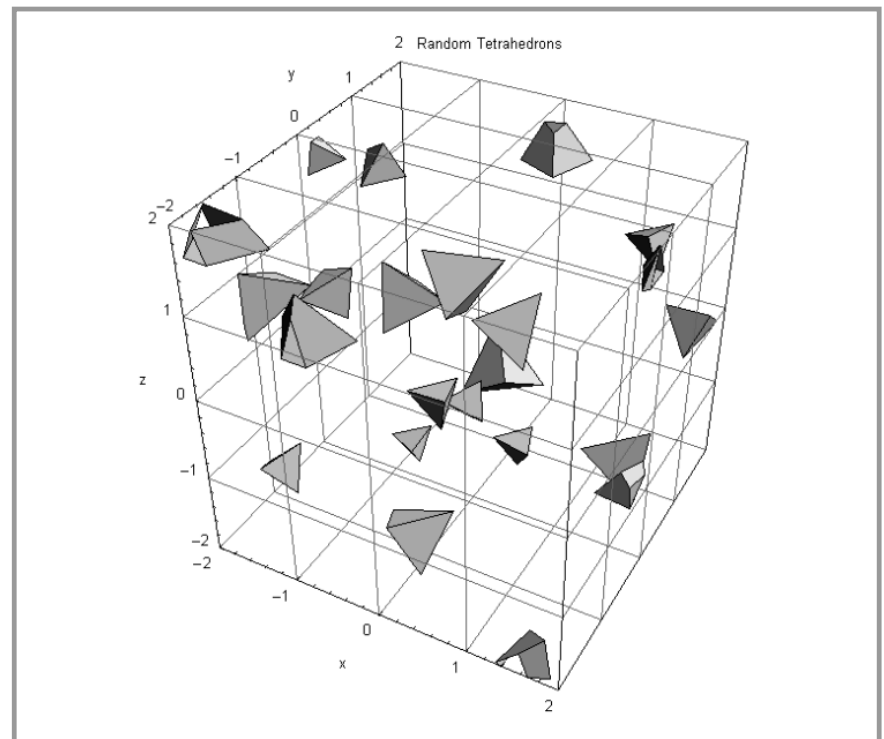


**Figure 1.** Simulation of tetrahedrons, isotropically uniformly randomly distributed in space, partly contained ( $N=23$ ) inside the cubic test volume. There is a certain distribution in size,  $a$ . The goal is to quantify  $f(a)$  based on stereological data. An assumption for the applicability of SAS is: The smallest chord length between any two tetrahedrons is greater than  $a_{\max}$  (the so-called quasi-diluted particle arrangement).

**Equation 1–7.**

$$\gamma_m(r) = \frac{\int_r^L a^3 \cdot \gamma(r,a) \cdot f(a) da}{\int_0^L a^3 \cdot f(a) da} \quad (1) \quad A_{vm}(r) = \frac{\int_r^L a^3 \cdot A_v(r,a) \cdot f(a) da}{\int_0^L a^3 \cdot f(a) da} \quad (2)$$

$$A_{um}(r) = \frac{\int_r^L a^2 \cdot A_u(r,a) \cdot f(a) da}{\int_0^L a^2 \cdot a(a) da} \quad (3)$$

$$2 \cdot \int_0^L r \cdot A_{vm}(r,a) dr = \int_0^L \gamma_m(r,a) dr = 1 \quad \int_0^L A_{vm}(r,a) dr = 1 \quad (4)$$

$$\int_0^L r \cdot A_{um}(r,a) dr = \frac{4\bar{V}}{S} \quad \int_0^L A_{um}(r,a) dr = 1 \quad (5)$$

$$\gamma_{app}(r,a) = \begin{cases} i1: & 1 - \frac{3.6742346r}{a} + \frac{4.525469r^2}{a^2} - \frac{1.8685497r^3}{a^3} \\ i2: & \frac{23.2697(r-a)^7}{a^7} + \frac{17.5039(r-a)^6}{a^6} + \frac{1.26265(r-a)^5}{a^5} \end{cases} \quad (6)$$

$$\frac{\partial^2 \gamma_{app}(r,a)}{\partial r^2} = \begin{cases} i1: & \frac{9.05094}{a^2} - \frac{11.2113r}{a^3} \\ i2: & \frac{977.329(r-a)^5}{a^7} + \frac{525.116(r-a)^4}{a^6} + \frac{25.2529(r-a)^3}{a^5} \end{cases} \quad (7)$$

the averaged functions with the density  $f(a)$  and the specific tetrahedron structure functions. Numerical methods allow  $f(a)$  to be determined in terms of experimental data sets. Therefore, approximations of the specific structure functions are elaborated. A simulation of a noised data set (where  $f(a)$  is the Rayleigh-distribution density) has been included.

**Connection between  $f(a)$  and stereological data**

The basic structure function in this field is the isotropised covariance  $C(r)$  [9]. The function  $C(r,a)$  of a single tetrahedron is connected with the SAS correlation function (CF)  $\gamma(r,a)$  of a single tetrahedron [5] via  $C(r,a) = V \cdot \gamma(r,a)$  [9]. Here,  $V$  is the tetrahedron volume. For a convex particle, the second derivative  $\gamma''(r)$  is connected with the chord length distribution (CLD) for isotropic uniform random (IUR) chords via  $A_u(r) = \bar{L} \cdot \gamma''(r)$ . The mean IUR chord length is  $\bar{L} = 4V/S$ , where  $S$  is the surface area of the figure. As to so-called v-chords, there is the connection  $A_v(r) = r \cdot \gamma''(r)$ , see [5, 10].

Let  $\gamma(r,a)$ ,  $A_v(r,a)$  and  $A_u(r,a)$  be the corresponding characteristic functions of the single tetrahedron. Then, the existence of any size distribution  $f(a)$  of the random edge length  $a$  leads to the mean functions  $\gamma_m(r)$ ,  $A_{vm}(r)$ ,  $A_{um}(r)$  (Equations 1–3).

As  $\gamma$ , and  $A_v$  disappear if  $a < r$ , lower integration limits  $a = r$  result. In equa-

tions (1-3),  $f(a)$  is one and the same function. It can be traced back to the mean (experimental) functions  $\gamma_m(r)$ ,  $A_{vm}(r)$  or  $A_{um}(r)$ . These are normalised by  $\gamma_m(0) = 1$  and Equations 4–5.

Approximations of the terms  $\gamma(r,a)$ ,  $A_v(r,a)$  and  $A_u(r,a)$  involved in equations (1-3) will be introduced in Section 2.1. This will be the deciding prerequisite for applying equations (1-3).

**The functions  $\gamma(r,a)$ ,  $A_v(r,a)$  and  $A_u(r,a)$**

The CF  $\gamma(r,a)$  is the basic function for determining of the tetrahedron. For  $0 \leq r < a/\sqrt{2}$ ,  $\gamma(r,a)$  has been determined analytically [11,12]. There are many other

intervals, one more complicated than the other. In order to represent  $\gamma$  in several other intervals belonging to  $a/\sqrt{2} \leq r \leq a$ , a series of trials leads to an approximation strategy based on three intervals  $i1, i2, i3$ ,

$$i1: 0 \leq r < a/\sqrt{2}$$

$$i2: a/\sqrt{2} \leq r \leq a$$

$$i3: a \leq r < \infty$$

In  $i3$ ,  $\gamma(r,a)$ . The result for  $i1$  and  $i2$  is (Equation 6).

Equation (6) is based on the power series of  $\gamma(r,a)$  at  $r = a$ . For details see [12] and Appendix. Consequently, the CLD for  $\mu$ -chords

$$A_u(r,a) \approx 4V/S \cdot \gamma_{app}''(r,a),$$

$$\bar{L} = a \cdot \sqrt{6}/9,$$

$$A_v(r,a) \approx a \cdot \sqrt{6}/9 \cdot \gamma_{app}''(r,a),$$

can be traced back to  $\gamma_{app}''(r)$ . This function (Equation 7) results from equation (6).

Finally, the CLD for v-chords, to be inserted into equation (2), is

$$A_v(r,a) \approx r \cdot \gamma_{app}''(r,a).$$

These characteristics are summarised in Figure 2.

**Numerical methods for solving the inverse problem**

For determining  $f(a)$  from equation (1), equation (2) or equation (3), standard methods exist (numerical and analytical [13,14]) in the theory of integral equations. A basic approach for solving equation (1) with respect to  $f(a)$  numerically is (Equation 8).

Equation (8) represents  $f(a)$  at certain selected sampling points  $a_1, a_1 < a_2 < a_3, \dots$

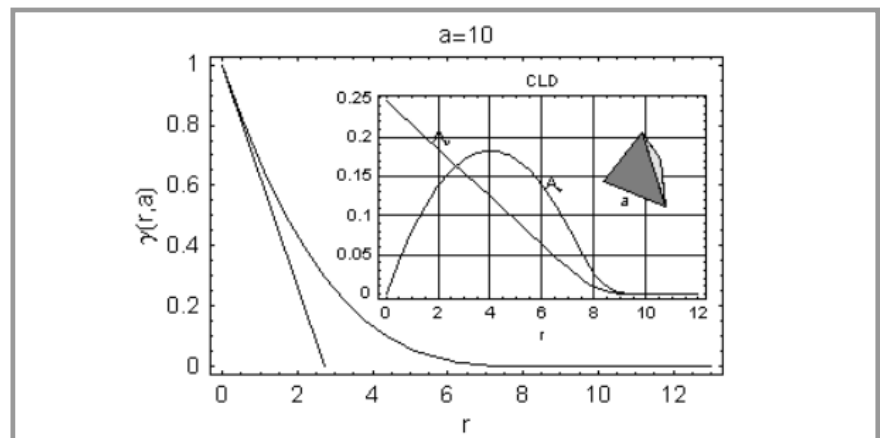


**Figure 2.** Specific functions  $\gamma(r,a) \approx \gamma_{app}(r,a)$ ,  $A_v(r,a)$ ,  $A_u(r,a)$  of a single regular tetrahedron in the case  $a = 10$ . The tangent of  $\gamma$  in  $(0,1)$  hits the axis of abscissa at  $r = a \cdot \sqrt{6}/9$ . This length is the first moment  $\bar{L}$  of  $A_u(r,a)$ . The particle diameter  $r = a = 10$  cannot be detected in an easy way, though all these functions disappear for  $a < r$ .

Equation 8, 9.

$$f(a) \approx g(a) = N_1 \cdot \delta(a - a_1) + N_2 \cdot \delta(a - a_2) + \dots + N_n \cdot \delta(a - a_n) = \sum_{i=1}^n N_i \cdot \delta(a - a_i) \quad (8)$$

$$\gamma_m(r) = N_1 \cdot a_1^3 \cdot \gamma(r, a_1) + N_2 \cdot a_2^3 \cdot \gamma(r, a_2) + \dots = \sum_{i=1}^n N_i \cdot a_i^3 \cdot \gamma(r, a_i) \quad (9)$$

by use of Dirac  $\delta$ -functions involving coefficients. Thus, equation (1) (and equations (2,3) also) can be traced back to a linear problem. Retyping equation (1), it follows (Equation 9).

As a consequence, the coefficients  $N_i$  and the set of known functions  $\gamma(r, a_i)$ , see equation (6), define the mean correlation function  $\gamma_m(r)$  at certain abscissas  $r_i$ ,  $0 \leq r_i \leq L$ . The non-negative real numbers  $N_i$  result from solving the approximation problem; see equation (9).

Application in a simulated case

Several simulations with assumed functions  $f(a)$  have been performed in order to demonstrate that practical application is feasible; see the following four steps.

1. Assuming  $f(a)$ : The Rayleigh-distribution density [15,16], (Equation 10) with  $\sigma = 5$ , has been inserted for one of the tests; see the filled plot in Figure 3A.
2. Simulation of  $\gamma_m(r)$ : Operating with equation (1),  $\gamma_m(r)$  (normalisation  $\gamma_m(0) =$

1) follows; see Figure 3A, thin line. A table  $\{r_j, \gamma_m(r_j)\}$ , 100 points in a typical case, results from equation (10). Insertion of the exact table leads back to  $f(a)$ .

3. Simulation of experimental conditions: A random number generator, set for 5% of noise, generates the random  $\gamma_m$ -values (see the points in Figure 3A). The  $r_j = \{0, 0.25, 0.50, \dots, 25\}$  have been considered as monotonously increasing exact lengths.

4. Determination of the  $N_i$ : By solving the approximation-problem equations (8,9) under the restriction of non-negative coefficients, certain coefficients  $N_i$  result. After correcting the normalisation of the coefficients, a pointwise function  $g(a_i)$  results. The inserted  $f(a)$  re-results. Both densities are compared in Fig. 3B.

The smaller the noise term, the better  $g(a_i)$  fits  $f(a)$ . From a series of experiments with different  $f(a)$  and varying noise terms, the limitations of the method (Section 2.2) have been detected: If the noise term is smaller than 5% and the number of data points  $\{r_j, \gamma_m(r_j)\}$  is at least four times the number of sampling points  $a_j$ , then  $f(a) \approx g(a_i)$  results.

Summary and conclusions

Aspects of determining the size distribution of tetrahedral particles – from linear intercept measurement or from scattering experiments via the SAS correlation function – have been developed. The approximation strategy for  $\gamma$  and  $A_{v,\mu}$  is based on combining a series expansion of  $\gamma(r)$  at  $r = a$  with the exact CF  $\gamma(r)$  in the first  $r$ -interval. Therefore, an elaborate  $r$ -interval splitting, inherent in any exact analytic representation of  $\gamma$  and  $A_{v,\mu}$ , has been avoided.

Based on equations (6,7) the particle size distribution density  $f(a)$  of tetrahedral particles has been considered. It can be obtained from data  $\{r_j, \gamma(r_j)\}$ , or  $\{r_j, A_{v,\mu}(r_j)\}$  or  $\{r_j, A_{v,\mu}(r_j)\}$  by numeric inversion of equations (1-3).

An exact analytic solution of the inverse problem,  $f(a)$  from  $\gamma(r)$  or  $f(a)$  from  $\gamma''(r)$ , has not yet been given for two reasons: On the one hand,  $\gamma(r)$  and  $A_{v,\mu}$  are approximations in the interval  $a/\sqrt{2} \leq r \leq a$ . On the other hand, a basic numerical method has been performed for the investigation of equations (1-3).

However, these two facts pose no restrictions for practical application. The fact that approximating formulas have been used in order to find the numerical solution of equations (1-3) does not present any restriction or limitation for practical applications. The data sets available in most cases are very rough, compared with the precision of the approximations which have been developed and applied.

Furthermore, the following may be supposed: Someday it will be possible to establish a general connection for all convex polyhedra, whose faces and vertices are of the same type, for all the Platonic solids.

Appendix

Series expansion of  $\gamma(r)$  at  $r = a$

The averaging procedure for determining the set covariance demands the consideration of two random direction angles,  $\theta$  and  $\phi$ . These angles of orientation are defined within the intervals  $0 \leq \phi < 2/3 \cdot \pi$ ,  $0 \leq \theta \leq \pi/2$ .

For determining and handling the series' expansion, a big expenditure is demanded. Even for the averaging procedure

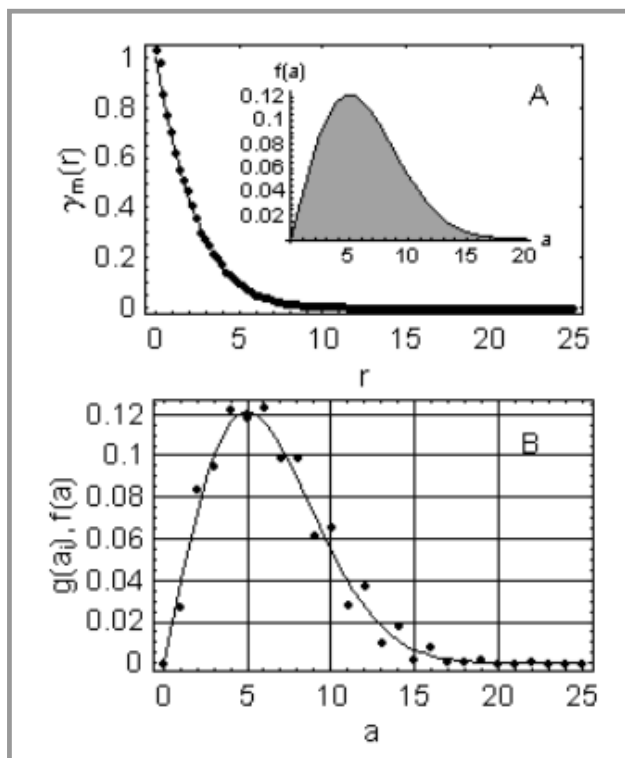


Figure 3. Example of a simulation, based on equations (1,6,8-10) A: The density  $f(a)$  has been selected for the simulation of  $\gamma(r)$  (101 data points, 5% noise) B: The unknown function  $g(a)$ , approximated by 25 points  $\{a_j, N_i \delta(a - a_j)\}$ , finally re-results.

( $r = const, r = a - \epsilon$ ), meticulous interval splitting is indispensable for handling the diversity of the cases of overlapping integrals [12,16]. Operating with the four basic overlapping volumes  $V_B(r, a, \phi, \theta)$ ,  $V_{AT}(r, a, \phi, \theta)$ ,  $V_I(r, a, \theta)$  and  $V_C(r, a, \phi, \theta)$ , eight parametric integrals  $R_1(r, a)$ ,  $R_2(r, a)$ , ...,  $R_8(r, a)$  have to be analysed. Then,  $V \cdot \gamma(r, a) = C(r, a) = R_1 + R_2 + \dots + R_8$ , with the set of equations (11) where nearly all the integration limits depend on each other and depend on  $r$ . For questions concerning the simplification of intermediate results, basic overlapping volumes  $V_B$ ,  $V_{AT}$ ,  $V_C$ ,  $V_I$ , the integration limits, the strategy of integration and the overlapping cases possible, please contact the author. Equation (11) is the starting point for performing the series expansion at  $r = a$  in question. The first two terms of the series expansion, resulting from equation (11), are equation (12).

Based on the form of equation (12), an approach involving three coefficients  $c_7$ ,  $c_6$ ,  $c_5$  (Equation 13) has been optimised for practical application within the inter-

#### Equation 11, 12, 13, 15 and 16.

$$\begin{aligned} R_1(r, a) &= \int_0^{\theta_E(r, a)} \int_0^{\phi_{ATB}(0)} V_B(r, a, \phi, \theta) \cos(\theta) d\phi d\theta \\ R_2(r, a) &= \int_0^{\theta_E(r, a)} \int_{\phi_{ATB}(\theta)}^{\phi_{BCAT1}(r, a, \theta)} V_{AT}(r, a, \phi, \theta) \cos(\theta) d\phi d\theta \\ R_3(r, a) &= \int_0^{\theta_E(r, a)} \int_{\phi_{BCAT2}(r, a, \theta)}^{\phi_{ATC}(\theta)} V_{AT}(r, a, \phi, \theta) \cos(\theta) d\phi d\theta \\ R_4(r, a) &= \int_0^{\theta_E(r, a)} \int_{\phi_{ATC}(\theta)}^{\phi_{ATBTC}(r, a, \theta)} V_C(r, a, \phi, \theta) \cos(\theta) d\phi d\theta \\ R_5(r, a) &= \int_0^{\theta_E(r, a)} \int_{\pi - \phi_{ATBTC}(r, a, \theta)}^{\frac{2\pi}{3}} V_C(r, a, \phi, \theta) \cos(\theta) d\phi d\theta \\ R_6(r, a) &= \int_{\theta_c}^{\theta_{\max}(r, a)} \int_{\phi_{ATCTB}(r, a, \theta)}^{\phi_{ATC}(\theta)} V_B(r, a, \phi, \theta) \cos(\theta) d\phi d\theta \\ R_7(r, a) &= \int_{\theta_c}^{\theta_{\max}(r, a)} \int_{\phi_{ATC}(\theta)}^{\phi_{ATB}(\theta)} V_I(r, a, \theta) \cos(\theta) d\phi d\theta \\ R_8(r, a) &= \int_{\theta_c}^{\theta_{\max}(r, a)} \int_{\phi_{ATB}(\theta)}^{\phi_{ATBTC}(r, a, \theta)} V_C(r, a, \phi, \theta) \cos(\theta) d\phi d\theta \end{aligned} \quad (11)$$

$$\gamma_a(r, a) = -\frac{13093(r-a)^5}{270\sqrt{2}a^5\pi} + \frac{425983(r-a)^6}{540\sqrt{2}a^6\pi} + O((r-a)^7) \quad (12)$$

$$\gamma_{app}(r, a) = c^7 \cdot \frac{(r-a)^7}{a^7} + c_6 \cdot \frac{(r-a)^6}{a^6} + c_5 \cdot \frac{(r-a)^5}{a^5} \quad (13)$$

$$\gamma_{app}(t) = \gamma(t) \quad \gamma_{app}'(t, a) = \gamma'(t) \quad \gamma_{app}''(t) = \gamma''(t, a) \quad (14)$$

$$\psi(h) = \int_0^\infty J_\nu^2(ha) \cdot h \cdot a \cdot f(a) da \quad f(a) = -2\pi \int_0^\infty J_\nu(ha) \cdot Y_\nu(ha) \cdot h \cdot \psi'(h) dh \quad (15)$$

$$\psi(h) = \frac{h^4 + 4h^2 + \sqrt{h^2 + 1} \cos(3 \tan^{-1}(h)) - 1}{(h^2 + 1)^2 \pi} \quad \psi'(h) = -\frac{4h^3(h^2 - 5)}{(h^2 + 1)^4 \pi} \quad (16)$$

val  $a/\sqrt{2} \leq r \leq a$ . A continuous, smooth approximation of the correlation function results, if the coefficients  $c_i$  in question fulfil three conditions at a selected transition point  $r = t = a/\sqrt{2}$ .

The solution of the resulting linear system, see equation (13,14), yields equation (6) and further equation (7), see Section Connection between  $f(a)$  and stereological data. Based on these coefficients, the maximum deviation between  $\gamma$  and  $\gamma_{app}$  is smaller than  $10^{-6}$ . For  $a = 10$ , the difference  $|\gamma'' - \gamma_{app}''|$  is smaller than  $5 \cdot 10^{-4}$ .

#### About the Titchmarsh transform

In some special cases (unfortunately the tetrahedron is not included here), the small-angle scattering intensity of a single particle is proportional to the square of the Bessel function of the first kind of index  $\nu$  (for example in the case of a uniform sphere, or an infinitely long cylinder). In this case, an integral transformation is known, which allows an analytic determination of the particle for several particle shapes [2,7,13].

The Titchmarsh transformation explicitly affiliates two functions  $f(a)$  and  $\psi(h)$  via the reciprocative connection (Equation 15) operating with the Bessel functions of the first and second kind,  $J_\nu(z)$  and  $Y_\nu(z)$ . Here,  $\psi'(h)$  is the first derivative. An example for equation (15) is, [13,14]: If  $\nu = 3/2$ ,  $f(a) = 4a^2 e^{-2a}$  and  $0 < h$ , then the equation 16 are obtained.

#### References

1. E. R. Weibel, Stereological Methods, Vol. 2, Academic Press, London 1980.
2. I. S. Fedorova, P. W. Schmidt, A General Analytical Method for Calculating Particle Dimension Distributions from Scattering Data, *J. Appl. Cryst.* **11** (1978) 405-411.
3. R. T. De Hoff, P. Bousquet, Estimation of the size distribution of triaxial ellipsoidal particles from the distribution of linear intercepts, *J. Microsc.* **92** (1970) 119-138.
4. J. Serra, Image Analysis and Mathematical Morphology, Academic Press, London, 1982.
5. A. Guinier, G. Fournet, Small-Angle Scattering of X-Rays, John Wiley, New York, 1955.
6. W. Gille, Size distribution of hemispheres from linear intercept measurement, *Laboratory report*, (75 pages), Martin Luther-University, Halle, 2000.
7. A. Erdélyi, W. Magnus, H. Oberhettinger, F.G. Tricomi, Higher Transcendental Functions, McGraw-Hill, New York, Toronto, London, 1953.
8. W. Gille, Diameter Distribution of Spherical Primary Grains in the Boolean Model from SAS, *Particle & Particle Syst. Characterization*, **12** (1995) 123-133.
9. D. Stoyan, W.S. Kendall, J. Mecke, Stochastic Geometry and Its Applications, Akademie Verlag, Berlin, 1987.
10. W. Gille, Chord length distributions and small-angle scattering, *Eur. Phys. J. B* **17** (2000) 371-383.
11. W. Gille, The small-angle structure functions of the single tetrahedron, *J. Appl. Cryst.* **36** (2003) 850-853.
12. W. Gille, The SAS structure functions of the tetrahedron, *Laboratory report 2002*, (84 pages), part 1: Basic equations and the first r-interval, part 3:  $g(r)$  for large  $r$  near  $r=a$ , Martin-Luther-University, Halle, 2002.
13. Wolfram Research Inc., Mathematica, version 4.2. Champaign, IL, 2002.
14. E. S. Wentzel, L. A. Owtscharow, Aufgabensammlung zur Wahrscheinlichkeitsrechnung, Akademie Verlag, Berlin, 1975.
15. W. Gille, Properties of the Rayleigh-distribution for particle sizing from SAS experiments, *NanoStructured Materials*, **11** (1999) 1269-1276.
16. C. G. Camko, A. A. Kulbas and O. I. Maritschew, Integrali i proiswodnie drobnowo porjadka i nekotorije priloschenija (*Nauka i Technika*, Minsk 1987).

Received 08.12.2004 Reviewed 10.02.2005